 https://doi.org/10.3311/PPci.40269

Periodica Polytechnica Civil Engineering, 69(3), pp. 1046–1061, 2025

Modified Component-based Model for Single and Double-angle Bolted Connections Used in Braced Steel Frames at Elevated Temperature

Ouissam Yessad[1], Abdelhak Kada[1*], Belkacem Lamri[1], Khalifa Al-Jabri[2], Muhammad Bilal Waris[2], Abdelhamid Bouchair[3]

[1] Laboratory Fire Safety Engineering of Constructions and Protection of their Environment LISICPE, Faculty of Civil Engineering and Architecture, Hassiba Benbouali University of Chlef, P.O.B. 78C, 02180 Ouled Fares, Chlef, Algeria
[2] Department of Civil and Architectural Engineering, Sultan Qaboos University, P.O.B. 33, P.C. 123 Al Khoudh, Muscat, Oman
[3] Université Clermont Auvergne, Clermont Auvergne INP, CNRS, Institut Pascal, F-63000 Clermont-Ferrand, France
[*] Corresponding author, e-mail: a.kada@univ-chlef.dz

Received: 22 February 2025, Accepted: 24 July 2025, Published online: 19 August 2025

Abstract

The article presents a modified component-based model for single and double-angle bolted connections used in braced steel frames under possible fire hazards. The study presents numerical models using finite element software ANSYS and a parametric analysis carried out on assemblies designed using Eurocode 3 considering bolt grade, number of bolts, angle size, and single/double angle. The analytical approach adopted for the component-based model (CBM) for the connection is used to predict the force-displacement relationships and the ultimate resistance for bolt shear failure and angle bearing. The numerical predictions showed excellent accuracy when evaluating the resistance of bolted angle steel connections at ambient and elevated temperatures. Also, the results revealed that the modified component-based model can effectively estimate the tensile resistance and the ultimate displacement of single and double-angle bolted connections. The modified component-based models can be used to investigate other failure modes like block shear fracture, bearing, and net section failure.

Keywords

angle connections, finite element analysis, tensile force, component-based model, elevated temperature, bolt shear, plate bearing

1 Introduction

The use of structural steel has gained momentum over the last decade, as the construction industry, designers, and developers sought to obtain sustainable and resilient contemporary building design [1–3]. Steel structures perform efficiently under earthquake loading, especially with braced frames to achieve resilience which made them the most suitable solution to seismic zones, such as Chlef, Algeria. This approach utilizes the bracing members as the main energy-dissipating element, while plastic shear in the links of steel braced frames is of paramount concern in the hierarchy of design [4]. Several design codes like Eurocode8 [5], AISC [6], and the RPA 2023 [7] seismic provisions, recognize them among the basic lateral load-resisting systems for steel structures [8]. In predominantly axially loaded members, web cover plates and angle steel connections continue to play a crucial role in modern construction, providing a combination of strength, flexibility, and aesthetic potential that is essential in contemporary architecture and engineering [9]. Although these structures are commonly designed to resist earthquake loadings at ambient temperature conditions, they are prone to collapse in a fire due to reduced strength and stiffness at elevated temperatures [10]. Experience from major events such as the collapse of the World Trade Centre (WTC) [11] and the research outcome of the Cardington full-scale fire tests [12] revealed that the design of the assemblies is most critical for the performance of the structure to prevent its collapse under fire. Previous research for structural steel fire resistance focused on investigating the mechanical behavior of individual members [13–15] or moment-resisting frames [16, 17]. These studies considered material degradation properties at elevated temperatures based on the ISO 834 fire curve [13] and focused on joint behavior at beam ends or on the beam-to-column

Cite this article as: Yessad, O., Kada, A., Lamri, B., Al-Jabri, K., Waris, M. B., Bouchair, A. "Modified Component-based Model for Single and Double-angle Bolted Connections Used in Braced Steel Frames at Elevated Temperature", Periodica Polytechnica Civil Engineering, 69(3), pp. 1046–1061, 2025. https://doi.org/10.3311/PPci.40269

connection. A review of the following research represents experimental and numerical works at ambient temperature. Kulak and Wu [18], Munse and Chesson [19] conducted tension tests on various angle connections to evaluate the load capacity, and failure modes including bearing, bolt shear, and angle net section failure. A numerical study for stainless steel on a single angle bolted to a gusset plate under tensile force and considering the net section rupture was conducted by Salih et al. [20] and design equations were proposed. Bernatowska and Ślęczka [21] carried out an experimental study on angle members connected by one leg with a single row of bolts, they found that the angle has three possible failure modes: net-section tearing, typical block tearing, and limited block tearing. Cavène et al. [22] proposed a new analytical approach to determine the initial stiffness of slotted cover plate components: one in bearing, one in bending, and one in shearing. Zhu et al. [23] tested 13 welded angle connections. and concluded that the failure load of the angles connected using the short leg and the ductility of all angle specimens were greater when the joints were welded with a symmetric arrangement. Abedin et al. [24] proposed new equations for the shear lag phenomenon and tension behaviour of single and double angles in welded connections taking into account connection eccentricity, connection length, gusset plate thickness, and members free length as parameters. Dhanuskar and Gupta [25] conducted full-scale tests on twelve double-bolt line connections in single-angle under tension and proposed an equation to predict the block shear capacity. To estimate the behavior of bolted connections at ambient and elevated temperatures, a comprehensive analytical approach such as the component-based method [26], [27] is much adapted to their analyses. The analytical component-based model has been effectively employed to characterize the performance of an isolated connection at high temperatures. Al-Jabri [28] utilized this approach to replicate the behavior of the flexible endplate connections under high-temperature conditions [29]. Sarraj [30] conducted finite element analyses on plates in bearings, and bolts in shear and also considered the friction at ambient and high temperatures. Sarraj proposed a model to predict the forces and deflections for the connections. Parametric studies were carried out using a bolt bearing on a plate, which did not adequately reflect the concentric or eccentric nature of the connections and the stress state under each state. Der and Wald [31] have investigated a component-based finite element model to design bolted lap joints at elevated temperatures under bearing, shear, and net section failure. Fischer et al. [32] presented a recent review on the behavior of simple shear connections under fire situations that summarized international experimental and numerical research on simple shear connections and indicated that further studies on single-angle connections are needed as they are widely used in the practice of construction, but their performance under fire has not yet been well characterized. Therefore, additional research on the behavior of each component of a fin and cleat plate connection exposed to the fire is necessary.

This paper presents a component-based model to predict the force-displacement relationship and the ultimate resistance for an individual bolt at elevated temperatures. The study used ANSYS to carry out a parametric analysis considering bolt grade, bolt numbers, and angle size, using single and double angles on assemblies designed according to Eurocode 3 [33, 34]. To further verify the accuracy of the model, it was compared with three failure modes: bolt shear fracture, angle failure in tension and the block shear fracture.

2 Design resistance for angles under tension

Design according to Eurocode 3 [34] is based on the number of angles (single or double) using specific formulas that consider bolt spacing bolt hole diameter edge distance, and the number of bolts for predicting the ultimate resistance of the connections.

2.1 Design resistance at ambient temperature

According to Eurocode 3 Part 1–8 [34] the net section resistance of single angles in tension connected by a single row of bolts in the direction of loading is estimated using Eqs. (1) or (2):

$$N_{u,Rd} = \frac{2\left(e_2 - 0.5d_0\right)tf_u}{\gamma_{M2}}, \tag{1}$$

$$N_{u,Rd} = \frac{\beta \cdot A_{\text{net}} \cdot f_u}{\gamma_{M2}}, \tag{2}$$

where: γ_{M2} is the partial safety factor with a Eurocode recommended value of 1.25, t represents the angle thickness, f_u the ultimate resistance, d_0 is the bolt hole diameter, β is a reduction factor dependent on the pitch p_1 and number of bolts.

The shear resistance of a bolt per shear plane is calculated using Eq. (3) and the bearing resistance per bolt using Eq. (4) according to Eurocode 3 [34]:

$$F_{v,Rd} = \frac{\alpha_v \cdot f_{ub} \cdot A_s}{\gamma_{M2}}, \tag{3}$$

$$F_{b,Rd} = \frac{K_1 \cdot \alpha_b \cdot f_u \cdot d \cdot t}{\gamma_{M2}}, \tag{4}$$

where α_v is 0.60, f_{ub} is the ultimate strength of the bolt, A_s is the tensile stress area of the bolt. d is the nominal bolt diameter, f_u is the nominal ultimate tensile strength of the angle, t is the thickness of connected material and γ_{M2} is the partial factor with the recommended value of 1.25. Parameters α_b and k_1 are determined considering mainly geometrical parameters as given below:

- Perpendicular to the direction of load transfer for edge and inner bolts, respectively:

$$k_1 = \min\left(2.8\frac{e_2}{d_0} - 1.7, 1.4\frac{p_2}{d_0} - 1.7, 2.5\right), \tag{5}$$

$$k_1 = \min\left(1.4\frac{p_2}{d_0} - 1.7, 2.5\right), \tag{6}$$

- in the direction of load transfer,

$$\alpha_b = \min\left(\alpha_d, \frac{f_{ub}}{f_u}, 1\right), \tag{7}$$

$$\alpha_d = \frac{e_1}{3d_0}, \tag{8}$$

$$\alpha_d = \frac{p_1}{3d_0} - 0.25 \text{ for inner bolts}, \tag{9}$$

where d_0 is the diameter of the bolt hole, f_{ub} is the ultimate strength of the bolt, f_u is the ultimate strength of the angle gusset, e_1 is the end distance, e_2 is the edge distance.

The design equations for calculating the block shear resistance is as follows:

$$V_{eff,1,Rd} = \frac{f_u \cdot A_{nt}}{\gamma_{M2}} + \frac{f_y \cdot A_{nv}}{\sqrt{3} \cdot \gamma_{M0}} \text{ for centric load}, \tag{10}$$

$$V_{eff,1,Rd} = 0.5\frac{f_u \cdot A_{nt}}{\gamma_{M2}} + \frac{f_y \cdot A_{nv}}{\sqrt{3} \cdot \gamma_{M0}} \text{ for excentric load}, \tag{11}$$

where: A_{nt} is the net area subjected to tension, A_{nv} is the net area subjected to shear, γ_{M0} is the partial safety factor equal to 1.

The design equation for the gusset plate resistance in tension according to Eurocode 3 Part 1–1 [35]:

$$N_{t,Rd} = \min\begin{cases} N_{pl,Rd} = \dfrac{A \cdot f_y}{\gamma_{M0}} \\ N_{u,Rd} = \dfrac{0.9 \cdot A_{\text{net}} \cdot f_u}{\gamma_{M2}} \end{cases}. \tag{12}$$

2.2 Design resistance at elevated temperature

Taking into account the mechanical properties of steel at high temperatures [33], the simplified rule for the design resistance in case of fire is derived from the one for a normal condition [34]. The resistance of the bolted angle gusset plate, at a specific elevated temperature θ is obtained by the above-mentioned resistances at 20 °C by the reduction factor for the yield strength of steel at temperature θ, reached at time t, $K_{b,\theta}$ is the reduction factor for bolts; and $K_{y,\theta}$ for steel determined at the appropriate temperature, their values of are listed in Table 1. The Eqs. (13)–(17) provides the bearing resistance, ultimate resistance, shear resistance of bolt and block shear resistance considering the effect of temperature.

$$F_{b,t,Rd} = F_{b,Rd} \cdot K_{b,\theta}, \tag{13}$$

$$N_{u,Rd,\theta} = N_{u,Rd} \cdot K_{y,\theta}, \tag{14}$$

$$F_{v,t,Rd} = F_{v,Rd} \cdot K_{y,\theta}, \tag{15}$$

$$V_{eff,1,Rd} = V_{eff,1,Rd} \cdot K_{y,\theta}, \tag{16}$$

$$N_{t,Rd} = N_{t,Rd} \cdot K_{y,\theta}. \tag{17}$$

3 Case of study

Angle gusset connections are denoted as cases of study from 1 to 5, Fig. 1 describes the connection according to the Eurocode 3 [34] configuration. Geometric parameters of studied cases are shown in Table 2 with details. Constant temperatures are uniformly distributed for room temperature θ = 20 °C, and temperatures, θ = 500 °C and 700 °C are chosen for an elevated temperature situation. The steel grade S235 (f_y = 235 MPa) was used for all gussets and angles. 16 mm diameter bolts of bolt grade 8.8 (f_{yb} = 640 MPa), and bolt grade 6.8 (f_{yb} = 480 MPa), with a typical value of elasticity modulus of 210 GPa.

Table 1 Properties of structural steel at high temperatures

Steel temperature (°C)	Reduction factors for steel at temperature θ_a, $K_{y,\theta}$	Reduction factors for bolt at temperature θ_a, $K_{b,\theta}$
20	1.000	1.000
500	0.780	0.550
700	0.230	0.100

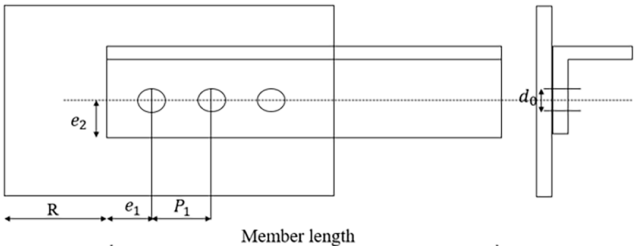

Fig. 1 Definition of symbols for angles connections (Case with 3 bolts)

4 Analytical Eurocode 3 results

Table 3 shows the shear strength for both bolt types without considering the safety factors. For temperatures of 500 °C and 700 °C, the shear strength of the bolts falls to 55% and 10%, respectively. While for steel connections start to lose their strength, with a percentage of 22% and 77% of their original capacity for 500 °C and 700 °C, respectively.

5 Finite element model

The numerical modeling is carried out using the finite element analysis software ANSYS APDL [36] to predict the mechanical behavior of the connection at ambient and elevated temperatures. SOLID185 element [37] was used to model all the connection parts (gusset, angle, and bolts). This element has eight nodes with three translational degrees of freedom at each node. It considers plasticity,

Table 2 Gusset angle connections description for all studied cases

Case of study	Angle size (mm)	Gusset plate dimensions (mm)	No. of Bolt	End distance 'e_1' (mm)	Pitch, 'p_1' (mm)	R (mm)
1	UA 100X100X10	200X200X15	1	50	-	100
2	UA 100X100X10	240X200X15	2	30	60	115
3	UA 100X100X10	260X200X15	3	35	75	120
4	2 UA 100X100X10	200X200X15	1	50	-	100
5	UA 70X70X7	240X100X10	2	30	60	120
6	UA 70X70X7	240X100X10	2	25	40	120

Table 3 Designed models at 20 °C, 500 °C, 700 °C according to EC3

Studied scenario	Shear résistance (kN) Eq. (3)		Bearing resistance (kN) Eq. (4)	Block shear Resistance (kN) Eqs. (10)–(11)	Gusset resistance (kN) Eq. (12)	Angle resistance (kN) Eq. (1)–(2)
	Bolt 8.8	Bolt 6.8				
T = 20°C						
Case (1)	75	64	320	199	705	575
Case (2)	150	128	160	238	705	276
Case (3)	225	191	240	398	705	244
Case (4)	150	128	320	199	705	1150
Case (5)	150	128	143	181	235	93
Case (6)	150	128	93	56	235	93
T = 500°C						
Case (1)	41	35	250	155	550	449
Case (2)	83	70	125	185	550	215
Case (3)	124	105	188	310	550	190
Case (4)	83	70	250	155	550	898
Case (5)	83	70	111	141	184	73
Case (6)	83	70	111	37	184	73
T = 700°C						
Case (1)	8	6	74	46	163	133
Case (2)	15	13	38	55	163	64
Case (3)	23	19	56	91	163	70
Case (4)	15	13	74	46	163	265
Case (5)	15	13	33	41	54	21
Case (6)	15	13	33	15	54	21

hyper-plasticity, stress stiffening, large deflection, and large deflection, and large strain features. A three-dimensional target element (TARGE170) was used to model the target area. TARGE170 is typically used to model 3D target surfaces for corresponding contact elements. A three-dimensional contact element (CONTA173) was used to model the flexible contact area. CONTA173 is typically used to simulate sliding and contact between a deformable contact surface and a three-dimensional target surface [38].

5.1 Material model and failure criteria

In this study, two distinct types of stress-strain relationships were employed to ensure the accuracy of the findings. For model validation, the material properties were determined using Engineering stress-strain curves, which accurately reflect the material's behavior under varying conditions. Simultaneously, the study incorporated the European standards, which are widely recognized and accepted in engineering practice. The stress-strain characteristics of steel are simulated based on Eurocode. The reduction factors proposed by Eurocode are applied to decrease Young's modulus, proportional limit, and yield strength of carbon steel at elevated temperatures [33]. For simplicity, the numerical simulation uses a material model that excludes the linear softening between 15% and 20% strain, which is included in the Eurocode material model for steel at both ambient and elevated temperatures. A bilinear material model was chosen for the bolts, assuming yielding occurs at the strain ε_p corresponding to the yield stress. The model also assumes a 25% elongation to fracture for the bolt, as indicated in ISO 898-1:2013 [39], with the ultimate strain for bolt grade 8.8 set at 12% and bolt grade 6.8 set at 8%. The adopted failure criterion for modeling steel plasticity is the von Misses yield criterion isotropic strain hardening. The Poisson's ratio is 0.3 and is considered not to change with temperature.

5.2 Contact Management and Boundary Conditions

The surface-to-surface contact model characterizes the complex interface between the bolt head, the bolt shank, the angle bolt hole, and the plate and the angle as indicated in Fig. 2 (a). Contact occurs when a contact element penetrates a target segment on a specific surface. This element supports custom friction, shear stress friction, and Coulomb friction. Additionally, the assembly allows the separation of bonded contacts to simulate interfaced elimination. The friction coefficient of 0.2 is used to represent sliding between contact surfaces. To keep the connection in the loading plane, the boundary and load conditions used in the numerical simulations take into account support with displacements U_x =0, U_y =0, and U_z =0 as well as the nodes on a line on the upper side of the plate with U_z =0 to avoid excessive displacement which could lead to unstable solution, and ensure that the load is transferred correctly between the connected parts. The load was applied as a function of time, at one leg angle nodes along the X- X-direction as indicated in Fig. 2 (b) because the axial load is usually assumed to act on the leg that is on direct contact of the other parts (only the tension force considered in this study). The non-linearity was handled using the Newton-Raphson incremental iterative method. The simulation ran smoothly, just like a genuine lab test, due to an accurate set of parameters that prevented localized strains or erroneous results.

5.3 Discretization and mesh sensitivity

The connection components were divided into several manageable sections to allow for the best possible meshing. A refined mesh with a size of 2 mm is applied to the

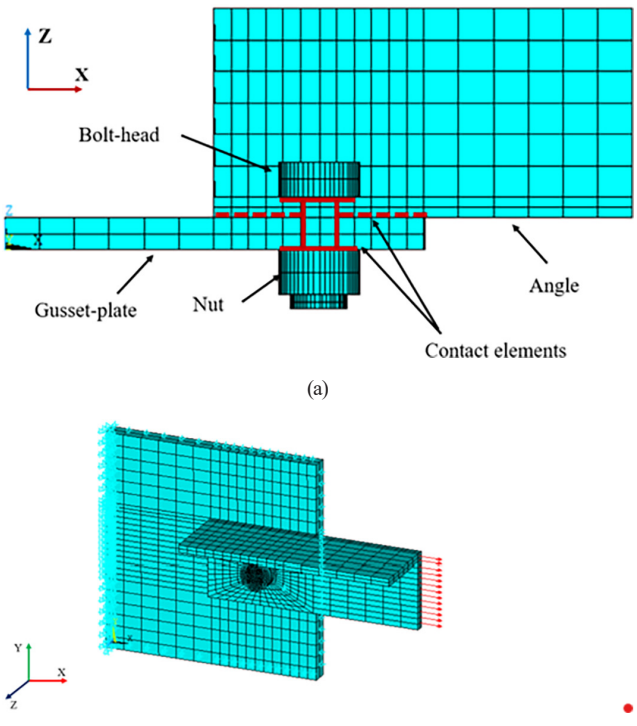

Fig. 2 Details of the FE modelling of the angle gusset connections (a) contact regions, (b) FE Model with applied load and boundary condition

bolts to ensure smooth contact between the bolts and the bolt holes. Since the bolt is designated as the master surface in the contact definition, a coarser mesh of 4 mm is used in the region around the bolt holes. In areas surrounding the bolt holes, the mesh size is set to 1/4 of the angle thickness. The plate and the angle are subdivided of 8 mm on the contact zones; In the non-contact zone of the connection, a coarser mesh was applied, with a size 2 times larger than the fine mesh used in the contact zone with two elements on the thickness. The mesh sensitivity study is presented in Table 4 using 1 mm, 1.5 mm, 1.75 mm, and 2 mm, respectively, size on the bolt. This mesh size was chosen as the best possible which still provides excellent agreement with the simulation results, which correspond to model No 4.

6 Validation of the numerical models

To validate the accuracy of the Finite Element (FE) model at both ambient and elevated temperatures. The required experimental data on the fire performance of bolted lap-joint tests were considered by Fischer et al. [40] in two failure modes: bolt shear failure at various temperatures, and from Ungkurapinan [41] for bolt bearing at ambient temperature. Fig. 3 illustrates a comparison between the load-displacement curves derived from the experiments and those from the Finite Element analysis. The displacement is measured as the axial deformation from the reference point at the constrained location to the second reference point at the applied load. The comparison shows that the FE model can predict the behavior of the connections with reasonable accuracy. The initial stiffness and ultimate capacity for the shear connections at ambient and elevated temperatures in Fig. 3 (a) are very well matched. The bearing mode in Fig. 3 (b) is also well represented.

Table 5 lists the critical experimental peak loads where they are compared with the results obtained from the FE analysis. It can be seen that the developed FE model is reliable for predicting the overall behaviour of bolted connections at ambient and elevated temperatures.

Table 4 Mesh sensitivity study

Model No	No of elements	Force (kN)	Displacement (mm)
1	9641	87.13	3.51
2	9552	87.18	3.52
3	8665	87.12	3.51
4	8420	87.11	3.51

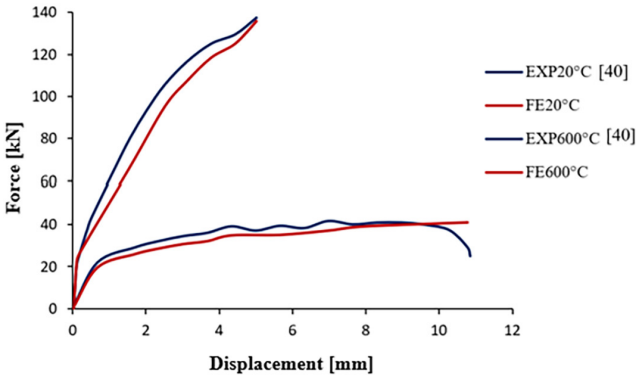

(a)

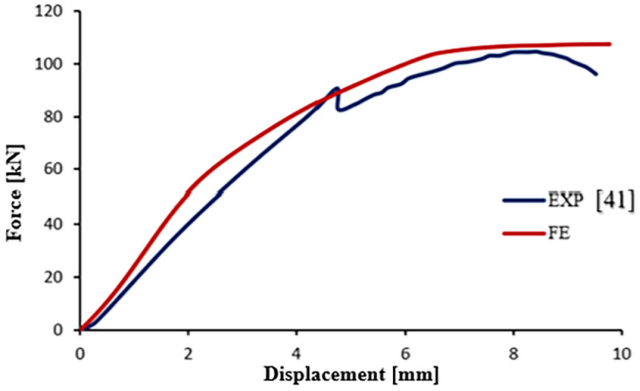

(b)

Fig. 3 Comparison of FE results with load-displacement curves from experimental tests (a) bolt shear mode, (b) bearing failure mode

Table 5 Comparison of critical values from tests and FE analysis

Tests specimen *N*	Experimental results (kN)	FE results (kN)	FE to experimental results ratio
Ungkurapinan (20 °C)	98	100	1.020
Fischer (20 °C)	137.3	135.8	0.987
Fischer (600 °C)	41	40	0.975

7 Parametric study

Parametric investigations were conducted using the numerical model to assess how changes in the angle dimensions, single/double angle, bolt type, and the total number of bolts impact the tension force-slip characteristics of single and double-leg bolted steel angle connections at elevated temperatures. The study compares these findings with the analytical-based model, both with and without considering the effect of friction.

7.1 Effects of the bolt grade

Fig. 4 depicts how the changes in bolt grade for Cases 1 to 4 influence the bolted angle connection response. Since, in Case 5, failure is governed by the rapture of the angle, it

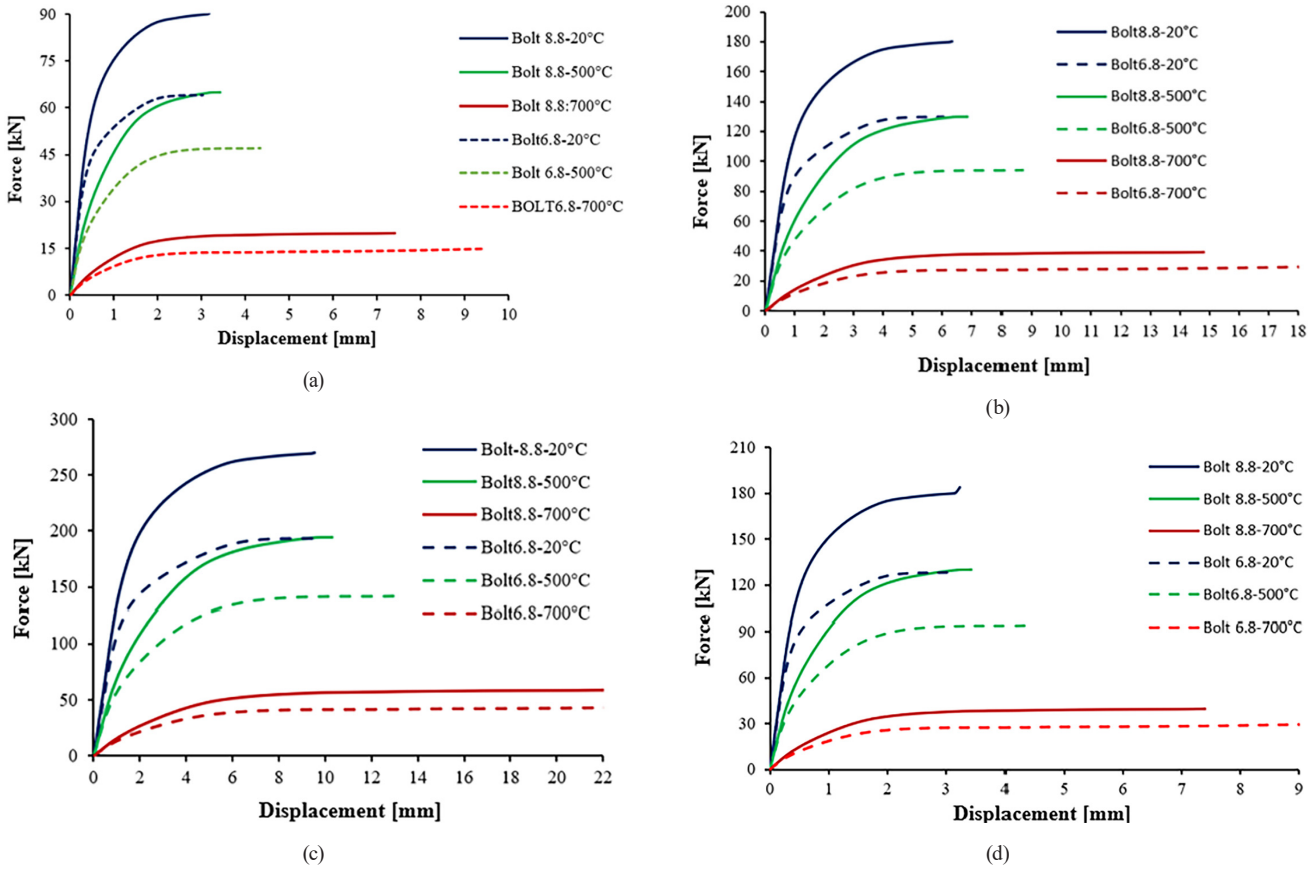

Fig. 4 Effect of bolt grade on failure in connection governed by bolt shear (Case: 1 – 4) (a) Case (1), (b) Case (2), (c) Case (3), (d) Case (4)

is not included in this section. Within the comparison set, the model replaced the G8.8 bolts in the connections with G6.8 bolts. The change of the bolt grade from bolt G6.8 with medium resistance to high strength G8.8 bolt shows the highest resistance. The values derived from the finite element analysis differ significantly from those specified in Table 3 of Eurocode 3, being 20% higher than those predicted by the code. This coincides well with the provision of a safety factor in EC3 that ensures the reliability of the structure. For example, in Case 1, the shear resistance value is 75 kN. In comparison, the value provided by finite elements is 87 kN, a percentage difference of approximately 16%.

7.2 Effect of bolt and angle number

The effect of the number of bolts on the connection behavior is considered using cases with one, two, and three bolts. The results are presented in Fig. 5 which shows that the load increases proportionally with the number of bolts. All the models with an UA 100X100X10 section (Case 1–4) failed by bolt fracture, so under the same temperature condition, the maximum load on the assembly with two and three bolts is approximately twice and three times the assembly with a single bolt.

Fig. 6 presents the results of the numerical models indicating that the deformation and stresses for Case 1, whether employing an HR bolt grade 8.8 or bolts grade 6.8 across all temperatures are well predicted. At ambient temperature, stresses are observed to be minimal at the plates and angles level but significant at the bolt level where the load is applied with the increase in temperature, the stresses begin to rise in the plates and the angles, especially in assemblies with 2 and 3 bolts (Cases 2 and 3), suggesting that shear is the dominant mode of failure at all temperatures. It is also observed that for Cases 1 and 4, the connection rotated after the failure, which was caused by the eccentricity between the gusset and the angles. In Cases 2 and 3 the rotation of the angle starts to decrease compared to connections with one bolt as also reported by Ungkurapinan [41]. Fig. 7 illustrates the load-displacement curves for Case 1 and Case 4, it shows how the double shear plan in the Case of the two angles impacts angle connection performance. It confirms that the resistance in Case 4 is more than twice that of Case 1.

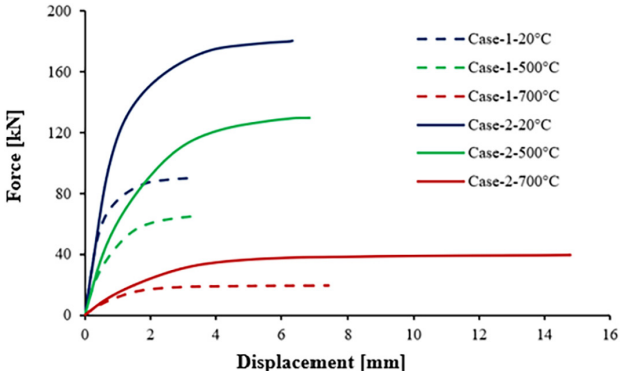

(a)

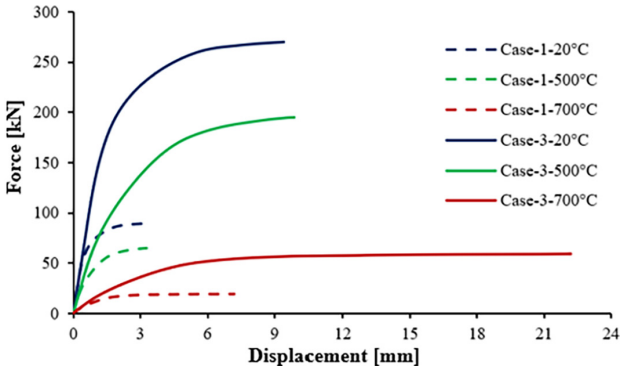

(b)

Fig. 5 Effect of the variation of bolt number (a) from two to one, (b) from three to one

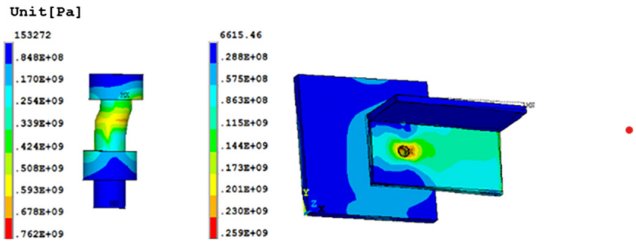

Fig. 6 Equivalent stress of the connection (Case 1) at 20 °C and at the failure load

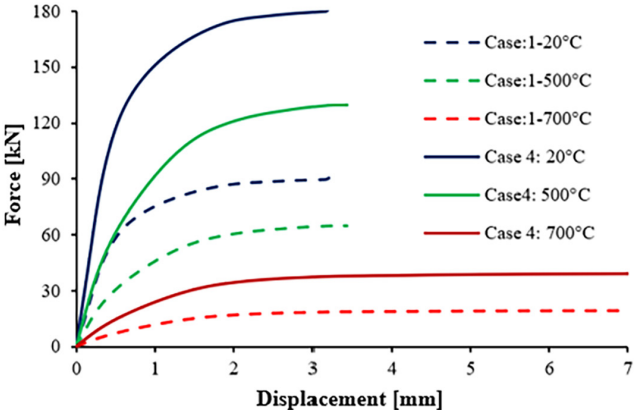

Fig. 7 Effect of the variation of the angle number from two to one

7.3 Effect of angle size

The finite element analysis in Case 5 shows that the connections with relatively smaller angle sections failed by tensile rupture of the steel angle at elevated temperature. The code predicted capacity of the UA 70 angle section as shown in Table 3 is 93 kN, which is relatively lower than the numerical prediction of 110 kN. As discussed earlier this is a difference of about 18%. Fig. 8 shows the effect of elevated temperatures on the tensile response of single angle bolted connections. As the temperature increases, it leads to decrease in the capacity. In this scenario, comparable declines in peak loads are noticed as the temperature rises. This correlation is linked to bolt and angle materials' reduced yield and ultimate tensile strength under higher temperatures.

Fig. 9 represents the result of the finite element model, which proves that the deformation state is within the angle for all temperatures with bolt grade 8.8 or bolt 6.8 grade, the stresses are low at the plate level and high at the angle level at the load application points which means that the mode of failure is by tension.

To understand the effect of the angle size on the connections, modifications were made to both the edge distance and the load transfer path (Case-6). The edge distance was reduced to limit the available shear area (e_2 = 25 mm), thereby increasing the likelihood of shear rupture along

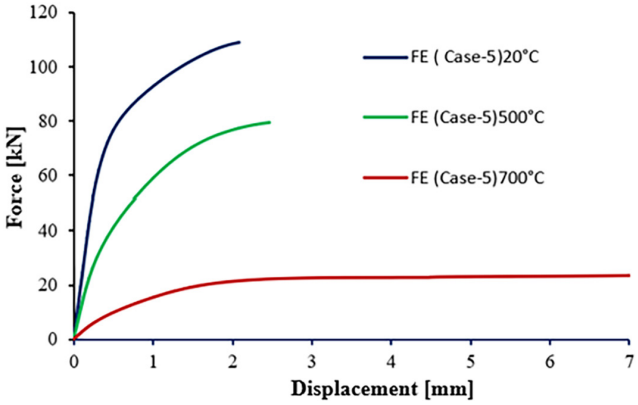

Fig. 8 Effect of temperature on small size angle

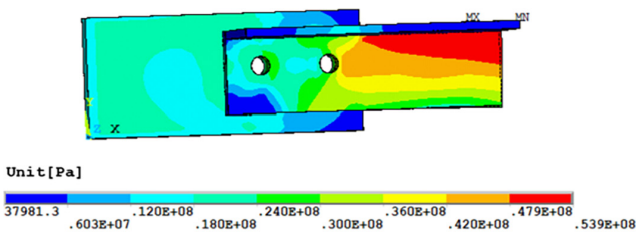

Fig. 9 Equivalent stress of the angle at 700 °C at the failure load

the expected failure plane. Adjustments were made to the load path to concentrate the stress flow so that, a combined tension and shear failure mechanism typical of block shear [42] takes place.

The predicted capacity of the connection, as determined by the design code, was evaluated against the finite element results to assess its accuracy in capturing the observed failure mode. The FE model consistently predicted higher connection capacities than the design code.

Fig. 10 presents the result of the finite element model showing block shear failure at ambient temperature.

At 500 °C, the failure mode begins to shift from block shear to tension failure in the angle, and by 700 °C, the dominant failure mode is entirely tension in the angle Fig. 11.

8 Modified Component-Based Model

This section focuses on the comparison of numerical results with the theoretical component-based model results, considering the two failure modes. The aim is to develop a modified component-based model based on [30] by considering the bearing of the gusset and angle, the shear of the bolt. For high-strength bolted connections grade 8.8, the model should also consider friction as shown in Fig. 12 (a), while ordinary bolts grade 6.8 can be considered frictionless as indicated in Fig. 12 (b) at ambient and elevated temperatures. This model treats the component as a set of elementary components, each represented by a spring whose behavior can be described mathematically.

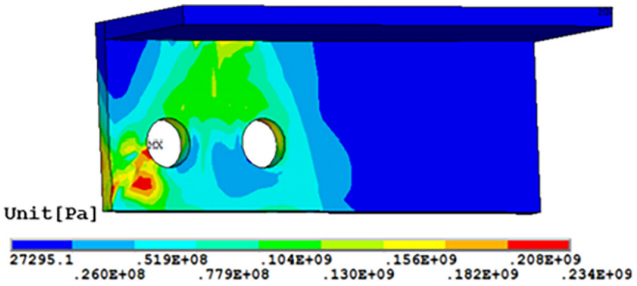

Fig. 10 Block shear failure at 20 °C (Case 6)

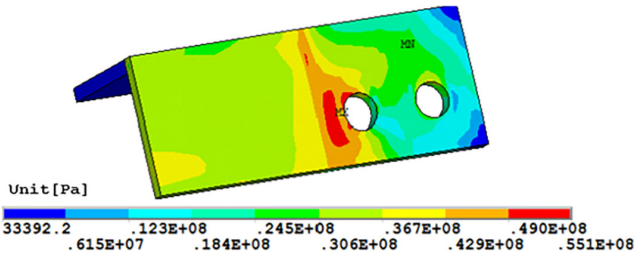

Fig. 11 Equivalent stress of the angle at 700 °C

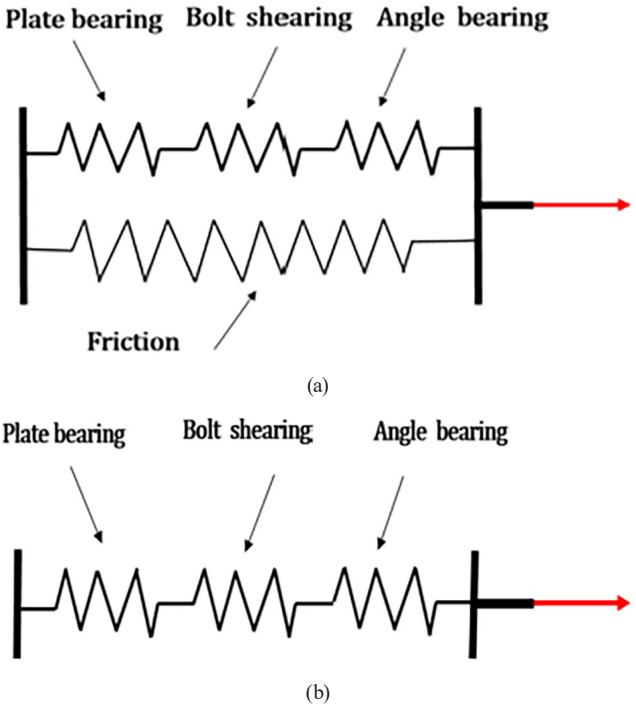

Fig. 12 Component Spring models for angle-plate connection (a) HR bolts grade 8.8, (b) ordinary bolts grade 6.8

The following discussion highlights the mechanism for the development of the component model to predict the ultimate displacement.

8.1 Gusset plate and angle components in bearing

Based on extensive experimental and numerical studies of bolted connections, Rex and Easterling [43] introduced bearing stiffness and related curves representing the relationship between bearing forces and corresponding displacements. Furthermore, Sarraj [30] highlighted that the load-bearing capacity of panels exposed to fire is very similar to that under normal conditions. They suggest accounting for fire conditions by incorporating reduction factors for material properties. Consequently, the initial bearing stiffness K_i, can be formulated as follows:

$$K_i = \frac{1}{\frac{1}{K_{br}} + \frac{1}{K_b} + \frac{1}{K_v}}, \tag{18}$$

$$K_{br} = 120 t f_y \left(d_b / 25.4\right)^{0.8}, \tag{19}$$

$$K_b = 32 E t \left(e_2 / d_b - 0.5\right)^3, \tag{20}$$

$$K_v = 6.67 G t \left(e_2 / d_b - 0.5\right). \tag{21}$$

Here, K_{br} represents the bearing stiffness of bolt holes; K_b and K_v denote the bending and shear stiffness of the bolt connection plate, respectively; G stands for the shear modulus of the gusset plate; E is the Young modulus, f_y the yield stress, d_b indicates the bolt diameter; t is the thickness of the bolt connection plate, and e_2 signifies the distance from the center of the bolt to the edge of the plate.

Rex and Easterling [43] provided bearing stiffness and correlation graphs showing the relationship between bearing forces and associated displacement, depending on substantial experimental and numerical investigations on bolt connections. Furthermore, it has been noted by Sarraj [30] that bolt holes exposed to fire exhibit bearing performance that is similar to that of normal settings.

$$\frac{F_b}{F_{b,Rd}} = \frac{\Psi\bar{\Delta}}{\left(1+\bar{\Delta}^{0.5}\right)^2} - \varphi\bar{\Delta}, \tag{22}$$

$$\bar{\Delta} = \Delta_b K_i \Big/ F_{b,Rd}, \tag{23}$$

$$F_{b,Rd} = \min\left(e_2; 2.76d_b\right) f_u t, \tag{24}$$

$$F_{b,Rd} = \begin{cases} 2\left(e_2 - 0.5d_0\right) t f_u \text{ for one bolt} \\ \beta \cdot A_{\text{net}} \cdot f_u \text{ more then one bolt} \end{cases}, \tag{25}$$

In this context, F_b and $F_{b,Rd}$ represent the bearing load and resistance of the plate according to Eq. (22) and the bearing force resistance for the angle in Eq. (25), respectively. $\bar{\Delta}$ and Δ_b signify the nominal and total deformation of bolt holes, respectively. Ψ and Φ represent the influential factors of fire temperatures, with their respective values provided in Table 6. The above bearing force-displacement relationship curve describes the development of the bearing pressure to reach its maximum force gradually as shown in Fig. 13 (a). The bearing capacity should be set at half the bot diameter (i.e., 0.50 d_b).

8.2 Force-displacement relationship of the bolt in the shear component

Sarraj's approach [30] contended that the adjusted Ramberg-Osgood equation provides a more accurate depiction of the force-displacement dynamics of a

Table 6 Correlation factors at different temperatures [°C] [30]

Temperatures [°C]	Correlative factors			Reduction factors
	Ψ	φ	Ω	
20	1.7	0.008	2.5	0.580
500	1.7	0.008	2	0.323
700	1.7	0.007	0.6	0.061

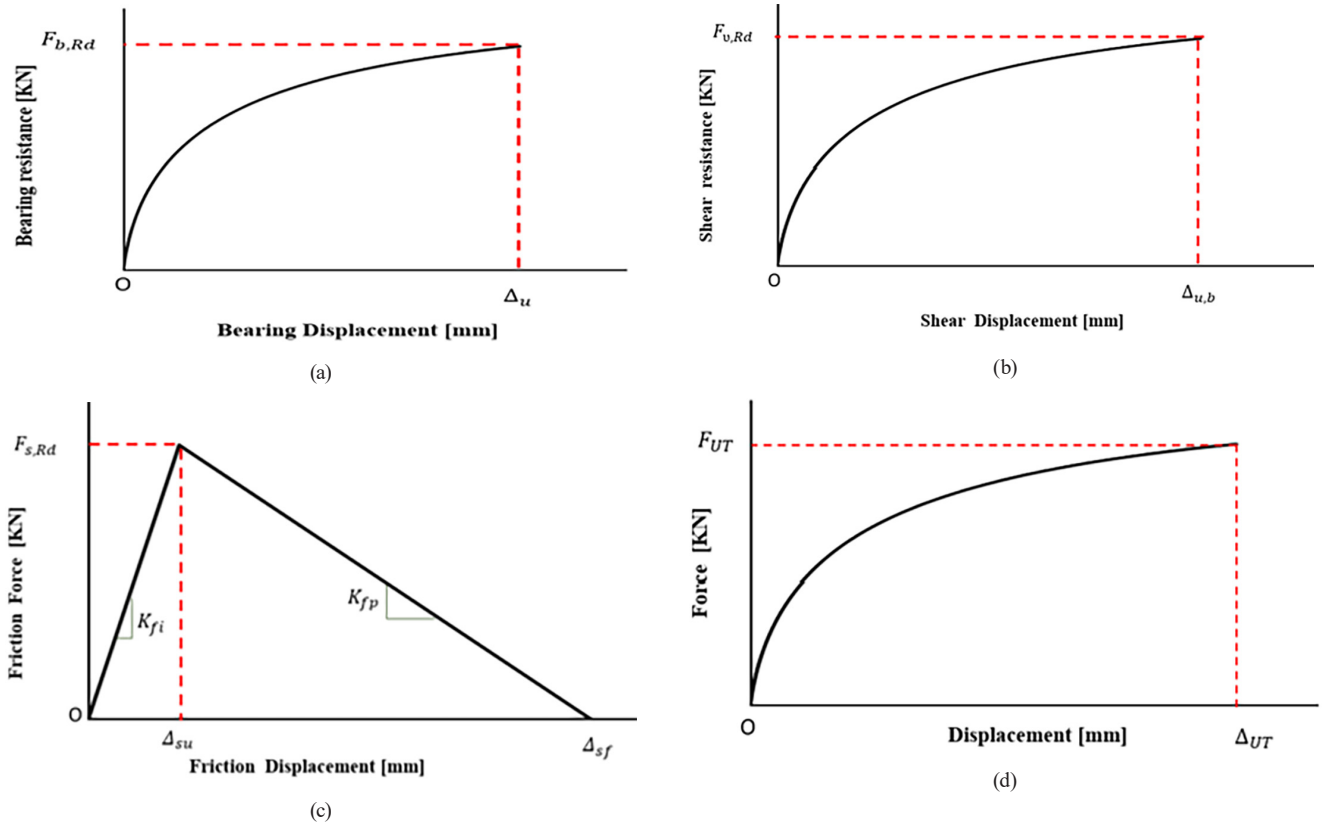

Fig. 13 Constitutive models for angle-bolted connection components (a) angle and plate in bearing, (b) bolt in shear, (c) angle and plate in slip, (d) angle and plate bolted connection

fire-exposed bolt under shear. The stiffness of the bolt is estimated by assuming that stress distribution is uniform across the shear plane of the bolt. The relationship between the bolt shear deformation Δ_υ and the level of shear force F_v is given by:

$$\Delta_\upsilon = \frac{F_v}{K_{\upsilon,b}} + \Omega\left(\frac{F_v}{F_{\upsilon,Rd}}\right)^n, \tag{26}$$

$$F_{\upsilon,Rd} = R_{f,v,b} \cdot f_{ub} \cdot A_s, \tag{27}$$

$$K_\upsilon = \frac{0.15GA_s}{d_b}. \tag{28}$$

Δ_υ represents the shear deformation of the bolt; F_v and $F_{\upsilon,Rd}$ denote the shear loads and ultimate shear loads of the bolt, respectively. $K_{\upsilon,b}$ stands for the shear stiffness of the bolt; Ω signifies the influential factors of fire temperatures; n (with n = 6) represents the correlation coefficient of the curve shape $R_{f,v,b}$ is the reduction factors of shear strength exposed to fire; f_{ub} represents the ultimate tensile strength of the bolt when exposed to fire; A_s is the tensile area of the bolt. The maximum displacement can be calculated by Eq. (26).

The whole shear force-displacement relationship curve of a typical bolt in consideration of the shear failure is illustrated in Fig. 13 (b).

8.3 Angle and gusset plate in slip

For plate angle bolted connections using high-strength bolts, the pre-tension force does not influence in the case of simple shear, but the sliding between the plates can generate frictional forces that may affect the structural response, based on the research results of [30], the slip load-displacement relationship curve between two plates can be simplified as a bilinear model, as shown in Fig. 13 (c). The main parameters in the plate friction component spring model include initial anti-slip stiffness, ultimate slip force, degradation stiffness, and maximum ultimate anti-slip displacement. Sarraj [30] proposed a triangular relationship between frictional force and displacement. The friction increases linearly from zero up to the maximum forces and then decreases linearly to zero. The maximum resistance is given by:

$$F_{s,Rd} = \frac{K_s \cdot n \cdot \mu \cdot F_{pc}}{\gamma_{M2}}, \tag{29}$$

$$F_{pc} = 0.7 \cdot F_{ub} \cdot A_s, \tag{30}$$

where; K_s is the groove factor and K_s = 1.0 for the standard hole; n is the number of forces transferring friction surfaces; μ is the friction factor given in the EC 3 with a value of 0.2, F_{pc} is the bolt pre-tightening forces. The total displacements, Δ_{sf} at zero resistance and Δ_{su} at the maximum resistance calculated using Eq. (31) and Eq. (32) are indicated in Fig. 13 (c)

$$\Delta_{sf} = \begin{cases} 16 \\ 16 - 0.3\left(t_1 + t_2 - 0.5\right) \\ 4 \end{cases} \begin{cases} \left(t_1 + t_2\right) < 20 \\ 20 \le \left(t_1 + t_2\right) \le 38.1, \\ 38.1 \le \left(t_1 + t_2\right) \end{cases} \tag{31}$$

$$\Delta_{su} = 0.18 \cdot d_b, \tag{32}$$

where t_1 and t_2 are the thicknesses of the gusset plates and angle respectively. The initial anti-slip stiffness K_{fi} and degradation stiffness K_{fp} are given by Eq. (33) and Eq. (34) respectively.

$$K_{fi} = \frac{F_{s,Rd}}{\Delta_{su}}, \tag{33}$$

$$K_{fp} = \frac{F_{s,Rd}}{\left(\Delta_{sf} - \Delta_{su}\right)}. \tag{34}$$

The overall load displacement behavior of the angle plate connection considering each component discussed earlier is shown in Fig. 13 (d). It is, therefore, possible to obtain the constituent model of the bolted connection. Within the models mentioned above the ultimate displacements can be calculated by the superposition of the series of spring components. The force-displacement curve of the angle plate connection is able to model the rapid decline after reaching ultimate loads.

9 Performance through the Component-Based Model and the FE model

9.1 Comparisons of the Component-Based Model and the FE model

To validate the simplified component-based model, comparisons between predictions from the finite element (FE) analysis, and the component-based model (with different configurations) are presented in Figs. 14 and 15. A good agreement can be observed between the finite element models and the component model. The approach demonstrates a reasonable prediction of the connection capacity under tensile load for both single and double bolted connection utilizing ordinary and high strength bolts.

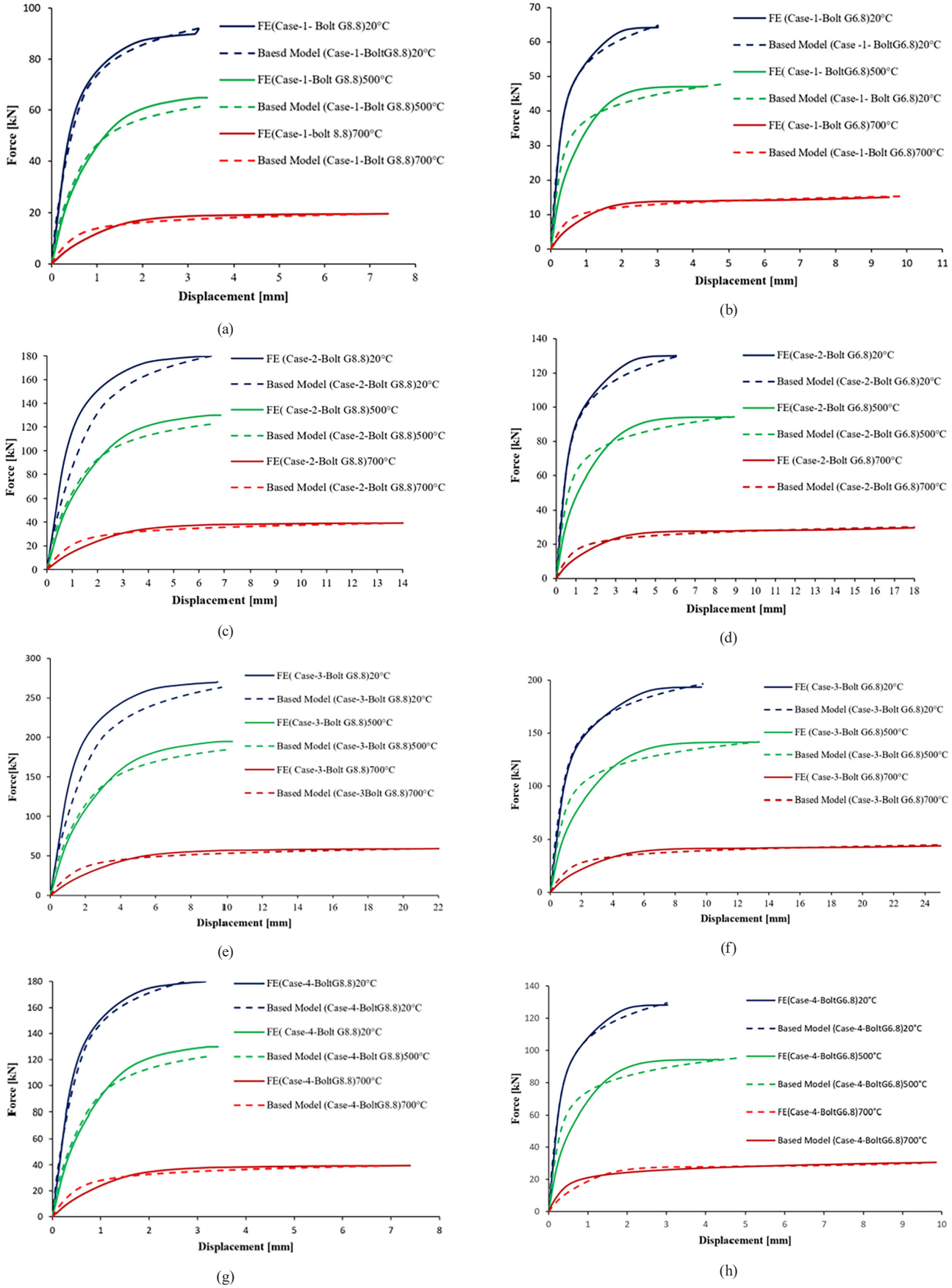

Fig. 14 Comparisons of FE and component-based model for assemblies with the same failure mode (Case 1, Case 2, Case 3, Case 4) (a) Case 1 (8.8 bolts), (b) Case 1 (6.8 bolts), (c) Case 2 (8.8 bolts), (d) Case 2 (6.8 bolts), (e) Case 3 (8.8 bolts), (f) Case 3 (6.8 bolts), (g) Case 4 (8.8 bolts), (h) Case 4 (6.8 bolts)

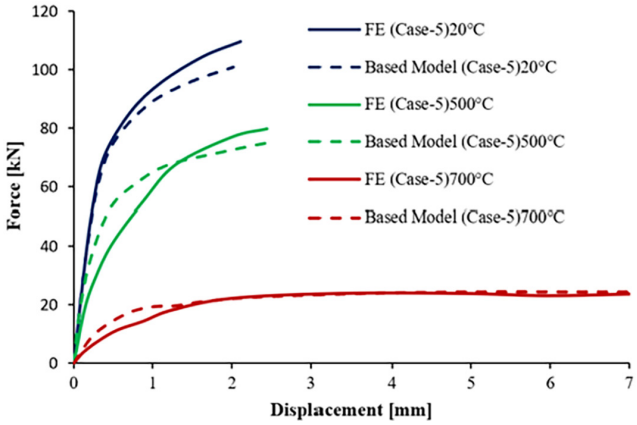

(a)

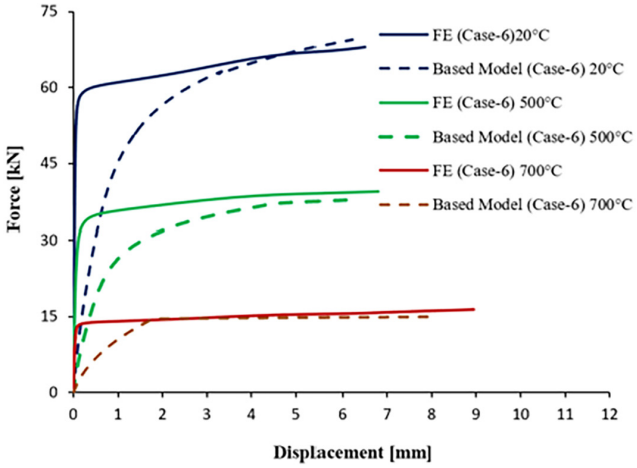

(b)

Fig. 15 Comparisons of FE and component-based model for (Case-5 and Case-6) (a) tension failure mode, (b) block shear failure mode

The component-based model is able to predict the performance of all six cases in terms of initial stiffness, nonlinear behavior, and ultimate loads with high accuracy. The performance of the model is also consistent across the elevated temperature.

9.2 Initial stiffness analysis

The initial stiffness K_i under the elastic regime before any significant plastic deformation indicates how the assembly behaves under the tensile load, which was defined as 2/3 of the plastic strength as previously determined by authors [44] and also in the European design code [34] and values for all cases are reported in Table 7. The table reports the values of the component-based model (CBM) and the finite element model (FE). It can be observed that for connections with bolts grade 8.8 (Cases 1 to 3) under shear failure mode, there is considerable difference in initial stiffness compared with bolts grade 6.8. In these connections which failed by the same failure mode the number of bolts did not significantly influence the initial stiffness. Conversely, a notable increase in initial stiffness was observed in the assembly subjected to double shear (Case 4), where the stiffness approximately doubled compared to those with bolts in single shear. In Case 5 and 6, although the initial stiffness is affected by the material properties and the geometry of the overall design of connections, it is not influenced by the changes in the bolts grade. At elevated temperatures, the assemblies result in lower initial stiffness, which indicates that the bolted joints offer weaker resistance, which could lead to larger deformations.

All bolted connections in the studied Cases (1 to 6) at ambient temperature show nonlinear force-displacement curves that start to yield due to plastic deformation. As the temperature increases, the response of the connections becomes more linear because the material loses stiffness and the connection has an overall loss of stiffness.

9.3 Ultimate force analysis

Table 8 lists the ultimate force derived from the analytical results and numerical analysis; the failure modes are defined as the model reaches its threshold. The ultimate strength is the maximum strength in the force-displacement curve.

10 Conclusions

This article analyzes and examines the temperature-dependent behavior of single and double-leg bolted steel angle connections under tension with bolts grande 8.8 and 6.8. The study developed and validated finite element models using ANSYS software to conduct a parametric study considering angle size, number of angles, bolt type, and number of bolts, which are designed according to Eurocode 3. The variations in these parameters have a significant impact on the ultimate resistance of the connection, affecting their failure modes, being bolt shear fracture or angle tensile failure.

The FE models, which incorporated geometric, material nonlinearities, and the contact between the components are validated against experimental results from the literature. A modified component-based model was proposed that could consider the interaction of all the elements in the connection and account for the material characteristics at elevated temperatures. The following key conclusion can be drawn from the work:

- A comparative analysis was performed based on the numerical results at each temperature, and the FE model showed higher capacities than the code predictions.

Table 7 Axial initial stiffness of joints at different temperatures

Studied scenario	$K_{ini,CBM}$ (kN/mm)		$K_{ini,FE}$ (kN/mm)		$K_{ini,FE}/K_{ini,CBM}$	
	Bolt 8.8	Bolt 6.8	Bolt 8.8	Bolt 6.8	Bolt 8.8	Bolt 6.8
20 °C						
Case (1)	96	93	115	95	1.197	1.021
Case (2)	99	96	114	97	1.151	1.010
Case (3)	89	85	124	107	1.393	1.258
Case (4)	211	192	240	194	1.137	1.010
Case (5)	118		126		1.067	
Case (6)	46		52		1.13	
500 °C						
Case (1)	46	31	46	32	1.000	1.032
Case (2)	54	60	48	41	0.888	0.683
Case (3)	48	43	51	37	1.062	0.860
Case (4)	88	76	96	78	1.090	1.026
Case (5)	47		51		1.085	
Case (6)	19		21		1.105	
700 °C						
Case (1)	13	13	16	13	1.230	1.000
Case (2)	14	13	11	13	0.785	1.000
Case (3)	13	13	17	15	1.307	1.153
Case (4)	19	17	23	17	1.210	1.000
Case (5)	10		11		1.100	
Case (6)	7		9		1.285	

Table 8 Ultimate Force of the connections with their failure mode at ambient and elevated temperatures

Studied scenario	Component-based model (KN)		*FE* (KN)		*FE*/CBM		Failure mode
	Bolt G8.8	Bolt G6.8	Bolt G8.8	Bolt G6.8			
20 °C							
Case (1)	87.1	64.8	87.8	64.1	1.008	0.989	Bolt shear
Case (2)	178.3	128.1	179.8	130.1	1.008	1.015	
Case (3)	259.4	194.4	269.7	193.6	1.038	0.995	
Case (4)	174.2	129.6	175.6	128.2	1.008	0.989	Bolt double shear
Case (5)	102.4		110.5		1.079		Tensile rupture
Case (6)	69.3		67.9		0.979		Block shear
500 °C							
Case (1)	62.7	46.6	64.8	46.1	1.033	0.989	Bolt shear
Case (2)	128.3	92.2	129.4	93.6	1.008	1.015	
Case (3)	186.7	139.9	194.1	139.3	1.039	0.995	
Case (4)	122.2	93.3	129.6	92.3	1.060	0.989	Bolt double shear
Case (5)	73.7		79.5		1.083		Tensile rapture
Case (6)	37.7		39.4		1.045		Block shear
700 °C							
Case (1)	20.0	14.9	20.1	14.7	1.005	0.986	Bolt shear
Case (2)	41.0	29.4	41.3	29.9	1.007	1.017	
Case (3)	59.6	44.7	62.0	44.5	1.040	0.995	
Case (4)	40.0	29.8	39.6	29.3	0.990	0.983	Bolt double shear
Case (5)	23.5		25.4		1.080		Tensile rapture
Case (6)	21.3		21.1		0.990		Tensile rapture

- The component-based model developed by Sarraj for the fin-plate under the axial load slip relationship was modified and utilized for the single and double-angle steel connections at ambient and elevated temperatures.
- The developed component-based model predictions matched well with the FE model.
- The model's efficiency defines each component's characteristics at any temperature and provides accurate estimates of the initial stiffness and ultimate strength of the connections.
- The component model, therefore, could be used for angle connection in braced steel frames with all types of connection bolts.

Acknowledgment
Authors wish to acknowledge the support of the Ministry of Higher Education and Scientific Research of Algeria (MESRS).

References

[1] Andrade, J. B., Bragança, L., Camões, A. "Steel sustainability assessment – Do BSA tools really assess steel properties?", Journal of Constructional Steel Research, 120, pp. 106–116, 2016. https://doi.org/10.1016/j.jcsr.2016.01.011

[2] Kosanović, S., Fikfak, A., Novaković, N., Klein, T. "Reviews of sustainability and resilience of the built environment for education, research and design", TU Delft OPEN Publishing, 2018. ISBN 978-94-6366-032-7 [online] Available at: https://books.bk.tudelft.nl/index.php/press/catalog/series/KLABS

[3] Mayar, K., Carmichael, D. G., Shen, X. "Resilience and systems – A review", Sustainability, 14(14), 8327, 2022. https://doi.org/10.3390/su14148327

[4] Bourahla, N., Hannachi, A. "GA-based optimisation of dissipative knee braced steel frames", In: Seismic Isolation, Energy Dissipation and Active Vibration Control of Structures, Antalya, Türkiye, 2024, pp. 145–155. ISBN 978-3-031-71048-3 https://doi.org/10.1007/978-3-031-71048-3_12

[5] British Standards Institution "BS EN 1998-1:2004 Eurocode8: Design of structures for earthquake resistance. General rules, seismic actions and rules for buildings", European Committee for Standardization, Brussels, Belgium, 2004. [online] Available at: https://www.confinedmasonry.org/wp-content/uploads/2009/09/Eurocode-8-1-Earthquakes-general.pdf

[6] AISC "Seismic provisions for structural steel buildings", American Institute of Steel Construction, Chicago, IL, USA, 2016.

[7] CTP "Algerian earthquake-resistant regulations", National Center of Applied Research in Earthquake Engineering, Algiers, Algeria, 2024. [online] Available at: https://www.tarekdata.com/FR/documents/normes/RPA-2024.pdf

[8] Black, R. G., Astaneh-Asl, A. "Design of seismically resistant tree-branching steel frames using theory and design guides for eccentrically braced frames", International Journal of Civil and Environmental Engineering, 8(2), pp. 206–213, 2014. https://doi.org/10.5281/zenodo.1090982

[9] Weisenberger, G., Engel, P., Grubb, K., Melnick, S. "Modern steel construction", American Institute of Steel Construction (AISC), [online] Available at: https://www.aisc.org/globalassets/modern-steel/archives/2024/december2024.pdf

[10] Sun, R., Huang, Z., Burgess, I. W. "The collapse behaviour of braced steel frames exposed to fire", Journal of Constructional Steel Research, 72, pp. 130–142, 2012. https://doi.org/10.1016/j.jcsr.2011.11.008

[11] Usmani, A. S., Chung, Y. C., Torero, J. L. "How did the WTC towers collapse: a new theory", Fire Safety Journal, 38(6), pp. 501–533, 2003. https://doi.org/10.1016/S0379-7112(03)00069-9

[12] Newman, G., Simms, I. "The Cardington fire tests", In: North American Steel Construction Conference, New Orleans, LA, Chicago, IL, USA, 1999, pp. 1–22, [online] Available at: https://www.aisc.org/globalassets/aisc/manual/15th-ed-ref-list/the-cardington-fire-tests_newman_1999.pdf

[13] Kada, A., Lamri, B., Mesquita, L. M. R., Bouchair, A. "Finite element analysis of steel beams with web apertures under fire condition", Asian Journal of Civil Engineering (Building and Housing), 17(8), pp. 1035–1054, 2016. [online] Available at: http://hdl.handle.net/10198/16492

[14] Kada, A., Lamri, B. "Numerical analysis of non-restrained long-span steel beams at high temperatures due to fire", Asian Journal of Civil Engineering, 20(2), pp. 261–267, 2019. https://doi.org/10.1007/s42107-018-0103-7

[15] Oribi, S. B., Kada, A., Lamri, B., Mesquita, L. "Behaviour of cellular steel beams at ambient and high-temperature conditions", Journal of Constructional Steel Research, 207, 107969, 2023. https://doi.org/10.1016/j.jcsr.2023.107969

[16] Merouani, M. R., Lamri, B., Kada, A., Piloto, P. "Mechanical analysis of a portal steel frame when subjected to a post-earthquake fire", Fire Research, 3(1), pp. 38–43, 2019. [online] Available at: https://materials.pagepress.org/fire/article/view/76

[17] Tartaglia, R., D'Aniello, M., Landolfo, R. "Response of seismically damaged steel reduced beam section joints under fire", Applied Sciences, 13(6), 3641, 2023. https://doi.org/10.3390/app13063641

[18] Kulak, G. L.,Wu, E. Y. "Shear lag in bolted angle tension members", Journal of Structural Engineering, 123(9), pp. 1144–1152, 1997. https://doi.org/10.1061/(asce)0733-9445(1997)123:9(1144)

[19] Munse, W. H., Chesson, E. "Riveted and bolted joints: Net section design", Journal of the Structural Division, 89(1), pp. 107–126, 1963. https://doi.org/10.1061/JSDEAG.0000869

[20] Salih, E. L., Gardner L., Nethercot, D. A. "Numerical study of stainless steel gusset plate connections", Engineering Structures, 49, pp. 448–464, 2013. https://doi.org/10.1016/j.engstruct.2012.11.032

[21] Bernatowska, E., Ślęczka, L. "Experimental and numerical investigation into failure modes of tension angle members connected by one leg", Materials, 14(18), 5141, 2021. https://doi.org/10.3390/ma14185141

[22] Cavène, E., Toussaint, É., Durif S., Bouchaïr, A. "An analytical model for the initial stiffness of bearing connections with slotted holes", Periodica Polytechnica Civil Engineering, 68(3), pp. 925–936, 2024. https://doi.org/10.3311/PPci.22310

[23] Zhu, H. T., Yam, M. C. H., Lam A. C. C., Iu, V. P. "The shear lag effects on welded steel single angle tension members", Journal of Constructional Steel Research, 65(5), pp. 1171–1186, 2009. https://doi.org/10.1016/j.jcsr.2008.10.004

[24] Abedin, M., Maleki S., Kiani, N., Shahrokhinasab, E. "Shear lag effects in angles welded at both legs", Advances in Civil Engineering, 2019(1), 8041767, 2019. https://doi.org/10.1155/2019/8041767

[25] Dhanuskar, J. R., Gupta, L. M. "Experimental investigation of block shear failure in a single angle tension member", International Journal of Steel Structures, 20(5), pp. 1636–1650, 2020. https://doi.org/10.1007/s13296-020-00398-2

[26] Abidelah, A., Bouchaïr, A., Kerdal, D. E. "Experimental and analytical behavior of bolted end-plate connections with or without stiffeners", Journal of Constructional Steel Research, 76, pp. 13–27, 2012. https://doi.org/10.1016/j.jcsr.2012.04.004

[27] Da Silva, L. S., Santiago, A., Real, P. V. "A component model for the behaviour of steel joints at elevated temperatures", Journal of Constructional Steel Research, 57(11), pp. 1169–1195, 2001. https://doi.org/10.1016/S0143-974X(01)00039-6

[28] Al-Jabri, K. S. "Component-based model of the behaviour of flexible end-plate connections at elevated temperatures", Composite Structures, 66(1–4), pp. 215–221, 2004. https://doi.org/10.1016/j.compstruct.2004.04.040

[29] Al-Jabri, K. S. "The behaviour of steel and composite beam-to-column connections in fire", Level (PhD), University of Sheffield, 1999. [online] Available at: https://etheses.whiterose.ac.uk/2997/

[30] Sarraj, M. "The behaviour of steel fin plate connections in fire", Level (PhD), University of Sheffield, 2007. [online] Available at: https://etheses.whiterose.ac.uk/id/eprint/3035/

[31] Der, B.,Wald, F. "Numerical design calculation of bolted lap joints at elevated temperatures", Fire Safety Journal, 147, 104202, 2024. https://doi.org/10.1016/j.firesaf.2024.104202

[32] Fischer, E. C., Chicchi, R., Choe, L. "Review of research on the fire behavior of simple shear connections", Fire Technology, 57(4), pp. 1519–1540, 2021. https://doi.org/10.1007/s10694-021-01105-1

[33] European Committee for Standarization (CEN) "EN_1993-1-2 Eurocode 3: Design of steel structures – Part 1-2: General rules – Structural fire design", European Committee for Standarization, Brussels, Belgium, 2005.

[34] European Committee for Standarization (CEN) "EN_1993-1-8 Eurocode 3: Design of steel structures – Part 1-8: Design of joints", European Committee for Standarization, Brussel, Belgium, 2005.

[35] European Committee for Standarization (CEN) "EN_1993-1-1 Eurocode 3: Design of steel structures – Part 1-1: General rules and rules for buildings", European Committee for Standarization, Brussel, Belgium, 2005.

[36] ANSYS "ANSYS Student® Academic research, (R 2.)", [computer program] Available at: https://www.ansys.com/academic/students/ansys-student

[37] ANSYS "ANSYS mechanical APDL element reference", [pdf] ANSYS Inc., Canonsburg, PA, 2011. [online] Available at: https://www.mm.bme.hu/%7Egyebro/files/vem/ansys_14_element_reference.pdf

[38] Moradi, S., Alam, M. S. "Finite-element simulation of posttensioned steel connections with bolted angles under cyclic loading", Journal of Structural Engineering, 142(1), 04015075, 2016. https://doi.org/10.1061/(ASCE)ST.1943-541X.0001336

[39] International Organization for Standardization (ISO) "ISO 898-1:2013 Mechanical properties of fasteners made of carbon steel and alloy steel – Part 1: Bolts, screws and studs with specified, property classes – Coarse thread and fine pitch thread", Geneva, Switzerland, 2013.

[40] Fischer, E. C.,Varma, A. H., Zhu, Q. "Experimental evaluation of single-bolted lap joints at elevated temperatures", Journal of Structural Engineering, 144(1), 04017176, 2018. https://doi.org/10.1061/(ASCE)ST.1943-541X.0001911

[41] Ungkurapinan, N. "A study of joint slip in galvanized bolted angle connections", Level (MSc), University of Manitoba, 2000. [online] Available at: http://hdl.handle.net/1993/6

[42] Jiang, B., Yam, M. C. H., Ke, K., Lam, A. C. C., Zhao, Q. "Block shear failure of S275 and S690 steel angles with single-line bolted connections", Journal of Constructional Steel Research, 170, 106068, 2020. https://doi.org/10.1016/j.jcsr.2020.106068

[43] Rex, C. O., Easterling, W. S. "Behavior and modeling of a bolt bearing on a single plate", Journal of Structural Engineering, 129(6), pp. 792–800, 2003. https://doi.org/10.1061/(ASCE)0733-9445(2003)129:6(792)

[44] Wald, F., Sokol, Z., Moal, M., Mazura, V., Muzeau, J.-P. "Stiffness of cover plate connections with slotted holes", Journal of Constructional Steel Research, 60(3–5), pp. 621–634, 2004. https://doi.org/10.1016/S0143-974X(03)00133-0